# 3D Time Domain Full Waveform Inversion with Reconstructed Wavefield

Chao Wang, David Yingst, Paul Farmer, Gary Martin, and Jacques Leveille, ION



## Abstract

Conventional full waveform inversion (FWI) has been an important tool for retrieving subsurface geology information. It has been successfully applied to real seismic data for both production and research purposes. The underlying theory has been well developed and the ultimate goal is to produce high-fidelity earth models by minimizing the difference between the acquired seismic data and computer synthesized data obtained by solving the wave equation exactly. In practice, FWI is still a beneficial but challenging method for updating the subsurface model parameters. A local optimization scheme is used to solve the minimization problem and it does not prevent convergence towards local minima because of the nonlinearity and ill-posedness of the problem. For example, it may suffer from cycle skipping problems if there is a lack of low frequency data. It may also converge to a local minimum from an inaccurate starting model.

To mitigate some of the issues associated with conventional FWI, we propose a new approach to time domain full waveform inversion with the reconstructed wavefield method (RFWI). RFWI replaces the exact solution of the wave equation in conventional FWI with an L2 approximation. RFWI estimates earth models and jointly reconstructs the source wavefield by minimizing a penalized objective function that includes both the data misfit and wave equation error. By extending the search space, RFWI offers potential benefits of avoiding cycle skipping and overcoming some of the problems with local minima. RFWI demonstrates more advantages in areas with strong velocity contrasts.

In this paper, we first present the theory and method of time domain RFWI. We also discuss the differences and similarities between conventional FWI and RFWI. Finally, the benefits and applicability of RFWI are demonstrated using two 3D field data sets.

## Introduction

Over the last decade, conventional full waveform inversion (FWI) has been an important method to build high fidelity earth models for seismic imaging (Lailly, 1983; Tarantola, 1984; Virieux and Operto, 2009). The goal is to estimate earth properties from the information acquired on the surface. It minimizes the misfit between acquired and synthetic data. FWI has been implemented in both the time and frequency domain (Sirgue and Pratt, 2004; Wang et al., 2013). However, it is a highly nonlinear, ill-posed problem and mitigating convergence to local minima is a severe challenge. For example, FWI may converge to a local minimum because of the lack of low frequencies in the recorded data or an inaccurate starting model.

To determine the misfit function for time domain FWI, the modeled data are extracted from the source wavefield generated by solving the wave equation, with an exact numerical solver using a finite difference scheme. In this paper, we propose a new approach to time domain FWI. This method, referred to as full waveform inversion with a reconstructed wavefield (RFWI), relaxes the constraint that the forward modeled data exactly solve the wave equation as in conventional FWI, and instead uses an L2 approximate solution. While conventional FWI searches for earth models such that the simulated source wavefield solves the wave equation exactly and the simulated data has the best match to the field data, RFWI optimizes over earth models and the source wavefield jointly to minimize the data misfit subject to the source wavefield being consistent with the wave equation in an L2 sense. The goal is to reconstruct a better source wavefield from the extended source instead of the original source signature for velocity update.

By adding the wave equation error as a penalty term to the original data misfit of conventional FWI, RFWI is a joint minimization problem that solves a penalized objective function. Instead of solving for one unknown, which is an earth model, now we are solving for two unknowns, a model and a forward propagated source wavefield. We reconstruct the source wavefield and estimate the model parameter in an alternating fashion. We first reconstruct the source wavefield from the extended source by minimizing the wave equation error and the data misfit. This least squares solution is computed by solving the normal equation. The reconstructed wavefield is then used for updating the model parameters with a gradient-based optimization method. Wavefield reconstruction inversion was originally introduced in the frequency domain (van Leeuwen and Hermann, 2013). Here we introduce our new approach and implementation of time domain RFWI, which is based on finite difference scheme and can be applied to 3D large-scale data sets. Compared to conventional FWI, RFWI is more computer-intensive.

Since RFWI forces the synthetic data to better fit the field data by expanding the search space, it may avoid cycle-skipping issues. RFWI mitigates some of the problems

with local minima that occur in conventional FWI when there is a lack of low frequency data or the initial model is inadequate. It also takes advantages of reflected seismic waves and reconstructs deeper portions of the model than conventional FWI that usually relies on diving waves. In general, RFWI demonstrates advantages in areas with strong velocity contrasts, which makes it a beneficial method for velocity model building in the presence of salt.

**Theory and Method**

Let's consider the general wave equation F[m]u=f, where m represents the subsurface model parameters, F[m] is the wave operator or D'Alembert operator, u is the forward propagated wavefield, and f is the source. Let S[m] denote the solution operator of the forward propagated wave equation. Then we have the conventional forward simulated source wavefield u = S[m]f.

Conventional FWI requires that we solve the wave equation exactly with the given source f. By replacing the forward propagated wavefield u with the exact solution S[m]f, we obtain the objective function for conventional FWI which uses the norm of the difference between the acquired field data and computer simulated forward modeled data that depends on the model m only

$$J[m] = \frac{1}{2}\left\| PS[m]f - d_0 \right\|_2^2,$$

where P is the restriction operator that records the source wavefield u at the receiver locations and $d_0$ is the acquired seismic data.

Unlike FWI, the idea of RFWI is to relax the constraint that u be an exact solution of the wave equation to an L2 approximation, by adding the wave equation error as a penalty term. Thus a new penalized objective function depending on the source wavefield u and the model m is introduced

$$\tilde{J}_\lambda[u,m] = \frac{1}{2}\left\| Pu - d_0 \right\|_2^2 + \frac{\lambda^2}{2}\left\| F[m]u - f \right\|_2^2,$$

with a penalty scalar $\lambda$. Source wavefield u should be forward going and therefore in the range of S, i.e. u = S[m]g for some source g. We call g the reconstructed or extended source. Note then that F[m]u=g and so the objective function of the extended source g and the model m can be redefined as

$$J_\lambda[g,m] = \frac{1}{2}\left\| PS[m]g - d_0 \right\|_2^2 + \frac{\lambda^2}{2}\left\| g - f \right\|_2^2.$$

While conventional FWI is an optimization problem only solving for the model m, this problem is a joint minimization of both g and m. To make it computationally feasible, we first minimize the above objective function with respect to g for a fixed m, which is the current model. Since the mismatch will be built into the reconstructed or extended source, the reconstructed source wavefield will be closer to the true wavefield for both reflections and refractions, which mitigates the issues of cycle skipping associated with conventional FWI. The least squares problem for reconstructing the source g is equivalent to solving the following normal equation

$$S^* P^* PSg + \lambda^2 g = S^* P^* d_0 + \lambda^2 f,$$

where * indicates the adjoint. The derivation details for reconstructing the extended source g can be found in Wang et al., 2016.

Once we have reconstructed the extended source g, we now can reconstruct the source wavefield u by forward propagating the extended source g. Then our next step is to minimize the objective function with respect to the model m. Now let's consider the following wave operator for a VTI system of two coupled second-order partial differential equations in terms of P-wave vertical velocity v, Thomsen parameters, $\varepsilon$ and $\delta$, assuming a constant density and zero shear velocity,

$$F[v] = \frac{1}{v^2}\partial_t^2 - \begin{pmatrix} 1+2\varepsilon & 1 \\ 1+2\delta & 1 \end{pmatrix}\begin{pmatrix} \partial_x^2 + \partial_y^2 & 0 \\ 0 & \partial_z^2 \end{pmatrix},$$

While fixing the anisotropy parameters, the gradient with respect to velocity can be calculated using

$$-\left\langle \frac{2}{v^3}\partial_t^2 u, S^* P^* (d_0 - PSf) \right\rangle.$$

where u is the reconstructed wavefield as described before, while FWI uses the conventional source wavefield instead. When the penalty scalar $\lambda$ is large enough, RFWI and conventional FWI converge to similar results. Thus the penalty scalar has to be chosen carefully to make RFWI produce favorable results and it may vary with iterations.

**Real Data Examples**

We first demonstrate an application of time domain RFWI to 3D marine data. This deep water ocean bottom seismic survey is located in the Green Canyon area of the Gulf of Mexico. The acquisition area was 160 $km^2$. This survey has 19901 sources with an interval of 50 m. Maximum offset used is 7000 m. The lowest frequency used from the observed data is about 5 Hz. The source signature was derived from the down-going wavefield on a zero offset section. The inversion proceeded with a single frequency band up to 8 Hz. The initial velocity model was built from tomography and its maximum depth is 12000 m. We first compare the gradients of conventional FWI and RFWI with this initial model. Figure 1(a) shows the gradient for conventional FWI using the initial model. Cycle skipping prevents it from getting any improvement except for the shallow sediment area. The deeper portion of the velocity model will not have a reasonable update because of limitations imposed by using the refraction data. However, the RFWI gradient using the initial model in Figure 1(b) has a clear base salt boundary at the right location. The subsalt gradient looks reasonable and follows the geology. The shallow updates for the sediment area should be comparable between the two methods as is observed. RFWI does improve the structure of the salt and the sediments below it.

Since the initial gradient demonstrates the potential benefits of RFWI, we now want to iterate and update the velocity model using RFWI. The inverted velocity model is shown in Figure 2(b) after 13 iterations of RFWI. The maximum updated depth is 12000 m. It demonstrates a reasonable shallow update above the salt. It also shows a deep update below 7000 m that follows the salt boundary and sub salt geology. The location of the salt body interface is well preserved by imposing a salt mask as in Figure 2. By improving the velocity, the offset gathers 3(b) after RFWI show improvement in flatness compared to the gathers 3(a) using the initial velocity for sediment area above 2707 m. To further evaluate the RFWI result, we generated the images using RTM and compare the subsalt imaging using the initial and inverted velocity models. Figure 4 shows zoomed images below the salt from 6035 m to 11883 m migrated with the two models. Comparing with the image using the initial model in Figure 4(a), the structures below the salt are improved with better continuity in the updated image 4(b), as indicated by the red rectangles.

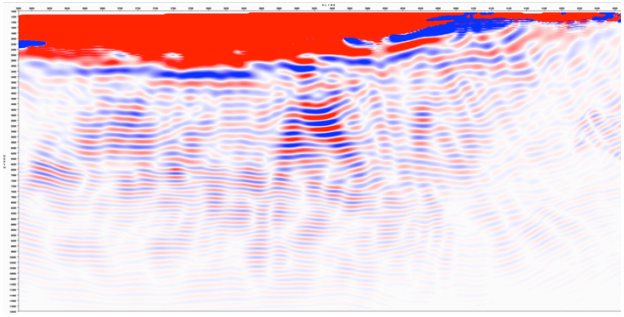

(a) Conventional FWI

(b) RFWI

Figure 1: gradients using initial model

Finally we present an application of time domain RFWI to another 3D streamer data. This narrow azimuth seismic survey is located in the Campeche area from offshore Mexico. Maximum offset was 6200m. We used 2280 sources with an interval of 500 m. The lowest frequency used from the observed data is about 4 Hz. A Ricker wavelet was used as the source signature to generate the synthetic data. The inversion proceeded with a single frequency band up to 8 Hz. The initial velocity model was built from tomography and its maximum depth is 6000 m. The initial velocity model is shown in Figure 5(a) and the inverted model is shown in Figure 5(b) after 10 iterations of RFWI. It demonstrates a reasonable shallow update above the salt. It also shows a deep update within, between, and below the salt bodies that follows the salt boundary and sub salt geology. By improving the velocity, the offset gathers 6(b) after RFWI show improvement in flatness compared to the gathers 6(a) using the initial velocity for sediment areas above the salt. To further evaluate the RFWI result, we generated the images using RTM and compare the stacks using the initial and inverted velocity models. Figure 7 shows seismic images migrated with the two models. Comparing with the image using the initial model in Figure 7(a), the structures above and below the salt bodies are improved with better continuity in the RFWI updated image 7(b) as indicated by the red rectangles. Data fitting is much improved with the updated model if we compare the synthetic data using the initial model in Figure 8(a) and the updated model in Figure 8(b) with the field data in Figure 8(c).

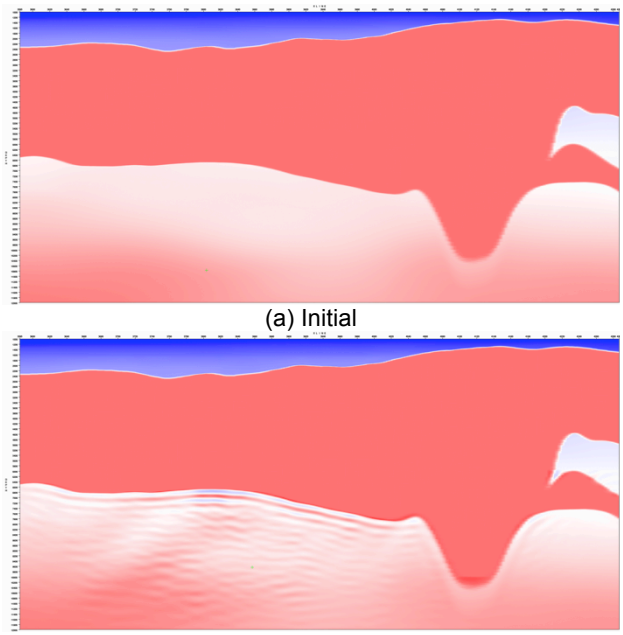

(a) Initial

(b) RFWI inverted

Figure 2: velocity models

**Conclusions**

We presented the method and applications of our proposed novel inversion method - time domain RFWI. RFWI helps avoid cycle skipping issues and overcomes some of the problems with local minima that occur in conventional FWI. It demonstrates more advantages in areas with strong velocity contrasts, which makes it a beneficial method for velocity model building with the presence of salt.

**Acknowledgments**

We would like to thank ION for permission to publish the results. The Campeche reimaging program data was reprocessed and reimaged by ION in partnership with Schlumberger, who holds data licensing rights. We also thank our colleagues for providing valuable help and support.

**References**

Lailly, P., 1983, The seismic inverse problem as a sequence of before stack migrations: Proceedings of the Conference on Inverse Scattering, Theory and Applications, Society for Industrial and Applied Mathematics, Philadelphia, 206–220.

Sirgue, L., and R. Pratt, 2004, Efficient waveform inversion and imaging: A strategy for selecting temporal frequencies: Geophysics, 69, 231–248, http://dx.doi.org/10.1190/1.1649391.

Tarantola, A., 1984, Inversion of seismic reflection data in the acoustic approximation: Geophysics, 49, 1259–1266, http://dx.doi.org/10.1190/1.1441754.

van Leeuwen, T., and F. Hermann, 2013, Mitigating local minima in full-waveform inversion by expanding the search space: Geophysical Journal International, 195, 661–667, http://dx.doi.org/10.1093/gji/ggt258.

Virieux, J., and S. Operto, 2009, An overview of full-waveform inversion in exploration geophysics: Geophysics, 74, no. 6, WCC1–WCC26, http://dx.doi.org/10.1190/1.3238367.

Wang, C., D. Yingst, J. Bai, J. Leveille, P. Farmer, and J. Brittan, 2013, Waveform inversion including well constraints, anisotropy, and attenuation: The Leading Edge, 32, 1056–1062, http://dx.doi.org/10.1190/tle32091056.1.

Wang, C., D. Yingst, P. Farmer, and J. Leveille, 2016, Full Waveform Inversion with Reconstructed Wavefield: 78th EAGE Conference and Exhibition. http://dx.doi.org/10.3997/2214-4609.201601538

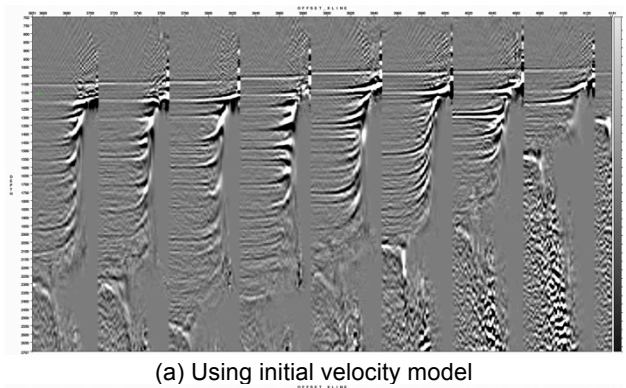

(a) Using initial velocity model

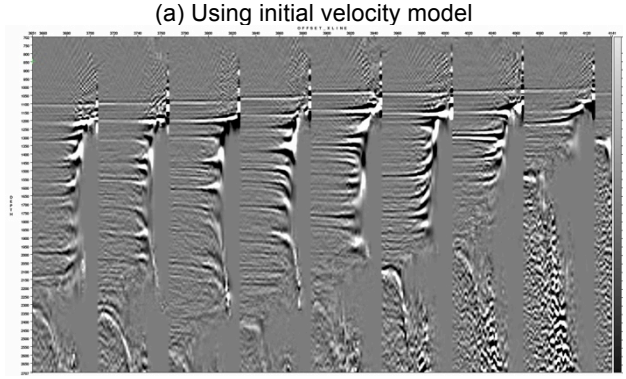

(b) Using RFWI inverted velocity model

Figure 3: offset gathers above the salt

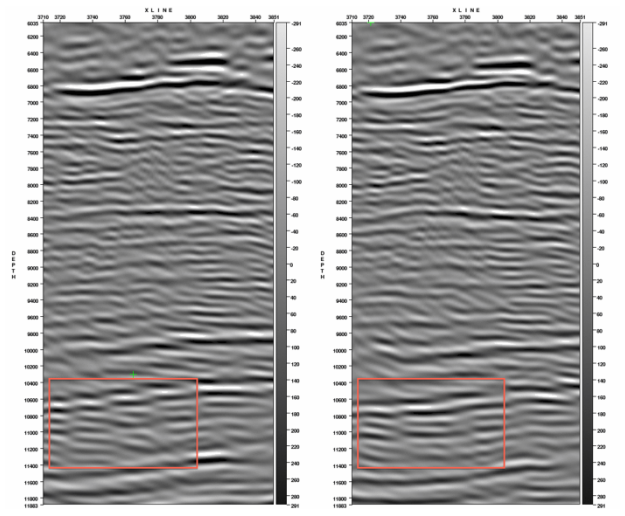

(a) Using initial model (b) Using RFWI model

Figure 4: migrated images for subsalt

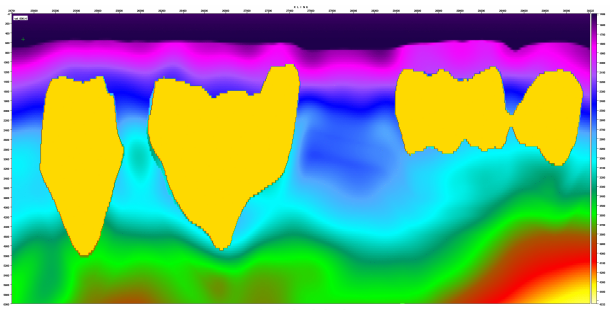

(a) Initial

(b) RFWI updated

Figure 5: velocity models

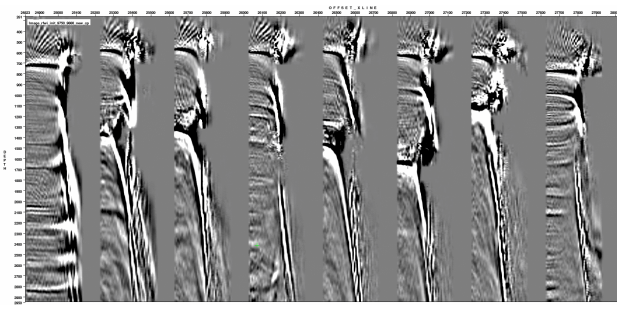

(a) Using initial velocity model

(b) Using RFWI updated velocity model

Figure 6: offset gathers

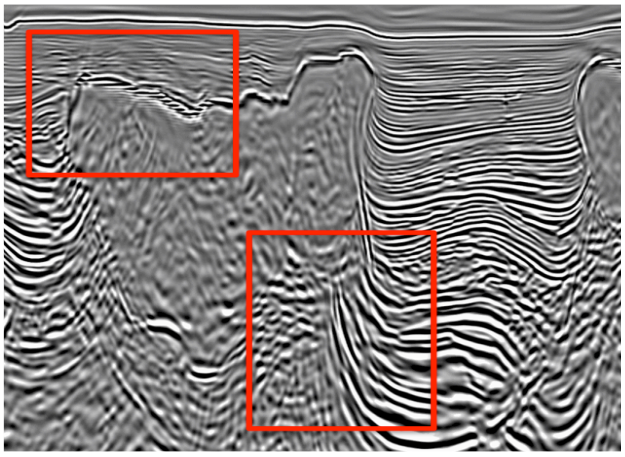

(a) Using initial velocity model

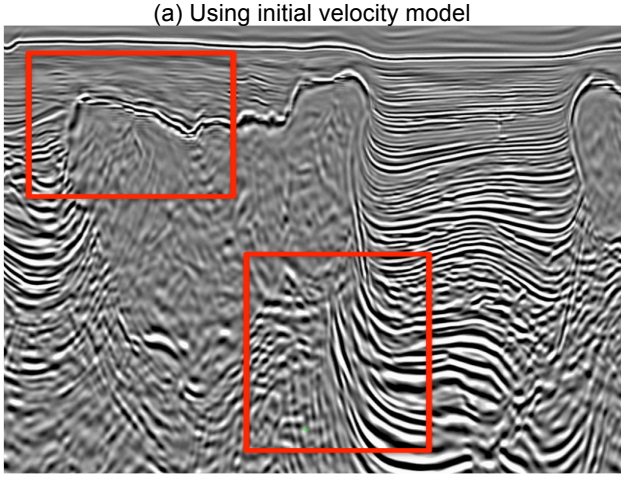

(b) Using RFWI inverted velocity model

Figure 7: migrated images

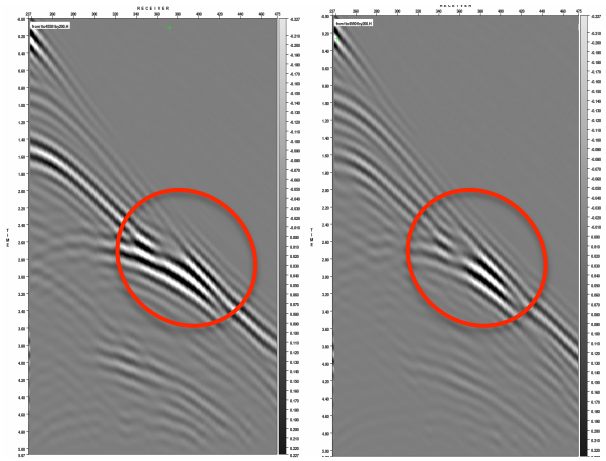

(a) Using initial model (b) Using RFWI model

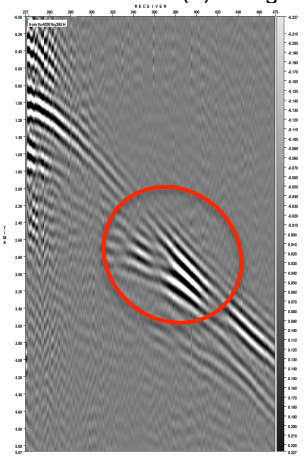

(c) Field data

Figure 8: shot gathers